Tellus (1979), 31, 340–350

The structure of the turbulent Ekman layer

By URBAN SVENSSON,[1] *Department of Water Resources Engineering, University of Lund, S-220 07 Lund, Sweden*

(Manuscript received October 24, 1978; in final form February 19, 1979)

ABSTRACT

A mathematical model is employed for analysing the structure of the homogeneous ocean surface layer. The model is verified against laboratory measurements of the fully developed channel flow and the wind-induced channel flow. Turbulence models of different complexities are used and discussed. An extension of the $k - \hat{\varepsilon}$ turbulence model to rotating flows is derived and tested.

The study indicates that a suitably chosen constant eddy viscosity is adequate for predicting the velocity and shear stress distributions in the Ekman layer. For transport of different chemical and biological species it is, however, necessary to know the detailed transport properties of the layer. Non-dimensional vertical distributions of different turbulence quantities, characterizing the Ekman layer, are therefore predicted and analysed. Rotational effects in the turbulence model are found to somewhat change the shear stress distribution in the deeper parts of the boundary layer.

1. Introduction

The objective of the present study is to examine the turbulent Ekman layer with the aid of a mathematical model. Interest is focused on the wind-induced Ekman boundary layer found in the well-mixed ocean surface layer. Special attention is given to the effect of the earth's rotation on mean flow and turbulent quantities. To be able to analyse this effect an idealized stationary boundary layer is assumed. A secondary objective is to provide general non-dimensional relationships for the mean velocities, Reynolds stresses, diffusion coefficients, etc. This kind of information is needed in general three-dimensional circulation models of the ocean and large lakes.

Earlier studies of the dynamics of the ocean surface layer, using advanced turbulence models (Mellor and Durbin, 1975; Marchuk et al., 1977), concentrate on the effect of density gradients. The mathematical formulation used in the present model is easily extended to the stratified case, but only homogeneous conditions will be treated in the present context. The reason for this is simply that the non-stratified situation should be fully explored before the stratified case is attempted. As will be emphasized later on there are several similarities between the considered problem and the Ekman layer in the atmosphere. The large body of knowledge gained about the atmospheric boundary layer (Mellor and Yamada, 1974, 1977; Zeman and Tennekes, 1975; Deardorff, 1970; Wyngaard, 1975) therefore represents a valuable source of information, when constructing mathematical models. Some of these studies have even considered the effect of rotation on the turbulence structure.

The mathematical formulation of the problem is given in Section 2 together with some basic assumptions made. In order to establish confidence in the model, it is in Section 3 applied to some laboratory flows, for which measurements are available. Section 4 contains the results concerning the ocean surface layer and Section 5 a discussion and some conclusions of the study. A derivation of a turbulence model with rotational effects is given in the Appendix.

2. The mathematical model

2.1. *Basic assumptions*

The study will restrict attention to horizontally homogeneous flows, which means that terms con-

[1] Present affiliation: Division of Water Resources Engineering, University of Luleå S-95187 Luleå, Sweden

 0040-2826/79/040340-11$02.50/0

taining gradients in the horizontal plane are neglected. It will also be assumed that no density gradients or mean vertical velocities are present. These assumptions constitute an idealized boundary layer. A further assumption is that Reynold's averaging of Navier–Stokes equations is a valid procedure.

2.2. *Momentum equations*

Within the assumptions made the momentum equations take the following form:

$$\frac{\partial U}{\partial t} = \frac{\partial}{\partial z}\left(-\overline{uw} + \nu\frac{\partial U}{\partial z}\right) + fV \tag{1}$$

$$\frac{\partial V}{\partial t} = \frac{\partial}{\partial z}\left(-\overline{vw} + \nu\frac{\partial V}{\partial z}\right) - fU \tag{2}$$

where z is the vertical space coordinate, positive upward, t the time coordinate, f the Coriolis parameter, U and V mean velocities in the x and y direction respectively, $\overline{uw}$ and $\overline{vw}$ the Reynolds stresses and ν the molecular kinematic viscosity.

The surface wind stress, $\boldsymbol{\tau}$, specifies the momentum flux at the surface, thus:

$$\left(-\overline{uw} + \nu\frac{\partial U}{\partial z}\right)_{z=0} = \frac{\tau_x(t)}{\rho} \tag{3}$$

$$\left(-\overline{vw} + \nu\frac{\partial V}{\partial z}\right)_{z=0} = \frac{\tau_y(t)}{\rho} \tag{4}$$

where ρ is the density of water. The present analysis assumes an infinitely deep ocean, with zero velocities at the lower boundary. To be able to apply a numerical model it is, however, necessary to specify a depth, D, where zero velocities are prescribed. Thus:

$$(U(t))_{z=-D} = (V(t))_{z=-D} = 0. \tag{5}$$

The depth of vanishing motion must, of course, be chosen large enough not to influence the predicted results in the region of interest.

2.3. *Turbulence model without rotational effects*

The turbulence model which does not take the Coriolis force into account is based on Prandtl's formula:

$$\nu_T = 1k^{1/2} \tag{6}$$

which states that the kinematic eddy viscosity, ν_T, can be determined from a length scale, 1, and a velocity scale, $k^{1/2}$. The velocity scale, $k^{1/2}$, is the root of the turbulent kinetic energy, k. Another assumption is that the rate of dissipation of turbulent kinetic energy, ε, can be related to k and 1 by the proposal by Chow (1945):

$$\varepsilon = C_\mu \frac{k^{3/2}}{1} \tag{7}$$

where C_μ is an empirical constant.

Eliminating 1 between (6) and (7) gives the following expression for ν_T:

$$\nu_T = C_\mu \frac{k^2}{\varepsilon} \tag{8}$$

which means that ν_T can be determined if k and ε are known. These variables are calculated from two transport equations, which can be derived in exact form from the Navier–Stokes equations and thereafter "modelled" to the following form:

Turbulent kinetic energy:

$$\frac{\partial k}{\partial t} = \frac{\partial}{\partial z}\left(\frac{\nu_{\text{eff}}}{\sigma_k}\frac{\partial k}{\partial z}\right) + P - \varepsilon \tag{9}$$

Dissipation of turbulent kinetic energy:

$$\frac{\partial \varepsilon}{\partial t} = \frac{\partial}{\partial z}\left(\frac{\nu_{\text{eff}}}{\sigma_\varepsilon}\frac{\partial \varepsilon}{\partial z}\right) + \frac{\varepsilon}{k}(C_1 P - C_2 \varepsilon) \tag{10}$$

where

$$P = \nu_T \left[\left(\frac{\partial U}{\partial z}\right)^2 + \left(\frac{\partial V}{\partial z}\right)^2\right] \tag{11}$$

and

$$\nu_{\text{eff}} = \nu_T + \nu. \tag{12}$$

Since the eddy-viscosity is defined as the ratio between the Reynolds stress and the shear it is now possible to formulate the following expressions for the Reynolds stresses.

$$-\overline{uw} = \nu_T \frac{\partial U}{\partial z} \tag{13}$$

$$-\overline{vw} = \nu_T \frac{\partial V}{\partial z}. \tag{14}$$

The constants appearing in (8), (9) and (10) are given in Table 1. For a detailed discussion of these constants and the underlying assumptions of this turbulence model see Launder and Spalding (1972, 1974) and Rodi (1978).

Table 1. *Constants in the turbulence model*

C_μ	C_1	C_2	σ_k	σ_ε
0.09	1.44	1.9	1.4	1.3

2.4. *Turbulence model with rotational effects*

Some of the more recent turbulence models (Zeman and Tennekes, 1975; So, 1977) have considered the Coriolis term in the Reynolds-stress equation and, in particular, the inclusion into the pressure-strain correlation. This approach is followed in the appendix where an extension of the $k - \varepsilon$ model to rotating flows is derived. It is found that the production term (11) and the expressions for the Reynolds-stresses (13) and (14) are modified as follows:

$$P = \nu_T \left[\left(\frac{\partial U}{\partial z} \right)^2 + \left(\frac{\partial V}{\partial z} \right)^2 \right] / (1 + R^2) \tag{15}$$

$$-\overline{uw} = \nu_T \left(\frac{1 + R \dfrac{\partial V}{\partial z} \Big/ \dfrac{\partial U}{\partial z}}{1 + R^2} \right) \frac{\partial U}{\partial z} \tag{16}$$

$$-\overline{vw} = \nu_T \left(\frac{1 - R \dfrac{\partial U}{\partial z} \Big/ \dfrac{\partial V}{\partial z}}{1 + R^2} \right) \frac{\partial V}{\partial z} \tag{17}$$

where

$$R = \phi_2 \frac{k}{\varepsilon} f \tag{18}$$

is a dimensionless quantity expressing the effect of rotation. The constant ϕ_2 is in the appendix found to be 0.4. Since k/ε is a timescale for the turbulence, R may be interpreted as the ratio between the time scale for turbulence and that for rotation. When this ratio is small R will be small and the model will return to the model for non-rotating flows. The expressions (15), (16) and (17) thus extend the regular $k - \varepsilon$ model to rotating flows. It is also interesting to note that Reynolds stresses do not by necessity change sign when the velocity gradients change sign. This means that an apparent negative eddy viscosity is possible.

3. Application to laboratory flows

In order to establish confidence in the mathematical model, predictions of the fully developed channel-flow and the wind-induced channel-flow are presented. The turbulence model for non-rotating flows is used since the earth's rotation is not expected to be of any importance in these flows. Further applications of the $k - \varepsilon$ model to boundary layer flows are reported by Singhal and Spalding (1975).

3.1. *The fully developed channel flow*

Important parameters specifying the flow are the mean velocity, $\bar{U}$, and the depth, D. An excellent series of measurements of this flow has been provided by Hussain and Reynolds (1975) and their profiles of velocity and eddy viscosity will be used for comparison. The flow studied may also be classified as the flow between two parallel walls. The upper boundary is thus a symmetry plane and therefore somewhat different from a channel flow with a free surface. Pressure gradients were not included in the mathematical formulation since they are assumed to be negligible for the ocean surface layer. In the present case it is of course the pressure gradient that drives the flow and this calls for a way of calculating it. For the steady state situation studied the following formula was employed:

$$\frac{\partial}{\partial t} \left(\frac{\partial p}{\partial x} \right) = C_p (\bar{U} - \bar{U}_p) \tag{19}$$

where $\bar{U}_p$ is the prescribed mean velocity and C_p a numerical constant. The formula produces a pressure gradient which in the steady state gives $\bar{U} = \bar{U}_p$, independently of C_p, since the left-hand side of the equation is then zero.

Boundary conditions for k and ε at the bottom are given by prescribed values, which are related to the calculated shear stress. At the upper boundary a zero flux condition is used, since this boundary is a symmetry plane. For further details concerning boundary conditions for the $k - \varepsilon$ model, see Launder and Spalding (1974). A comparison between measured and calculated profiles of velocity and eddy viscosity is shown in Fig. 1. The agreement is impressive and gives support to the mathematical model.

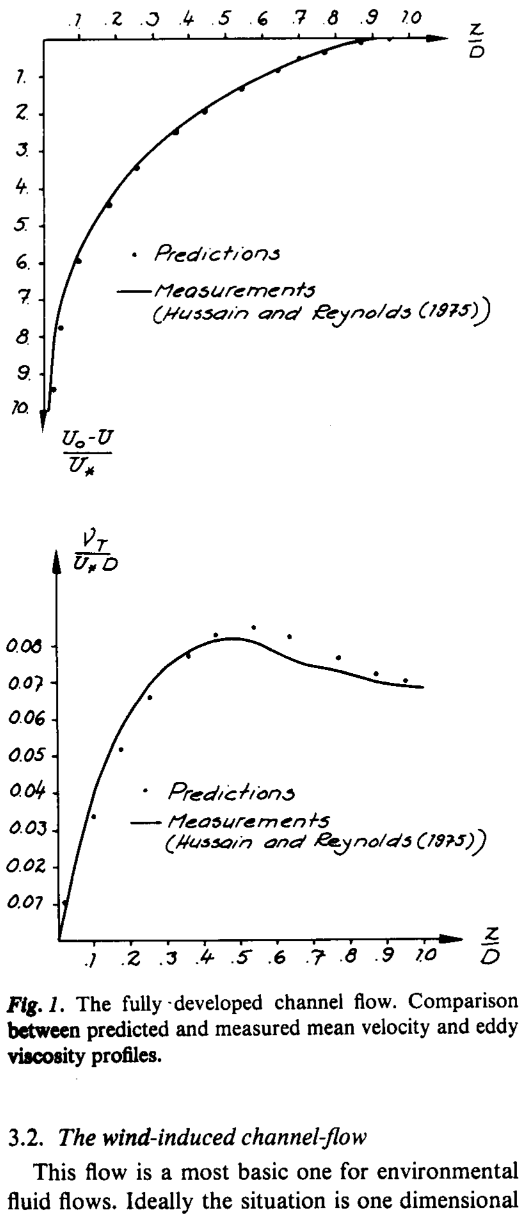

Fig. 1. The fully-developed channel flow. Comparison **between** predicted and measured mean velocity and eddy **viscosity profiles.**

3.2. *The wind-induced channel-flow*

This flow is a most basic one for environmental fluid flows. Ideally the situation is one dimensional with a surface stress and an adverse pressure gradient. The return flow at the bottom, driven by the pressure gradient, ensures that mass conservation is fulfilled. Depending on the wind stress the surface can be hydrodynamically smooth or rough. Measurements of the velocity profile have been reported by Baines and Knapp (1965) and these will be used for comparison. A calculated velocity profile, based on an experimentally determined eddy viscosity distribution, has been given by Barannik et al. (1977). Since this profile represents experimental data it will also be used for comparison. The pressure gradient was calculated using formula (19) with $\bar{U}_p = 0$. Boundary conditions for k and ε were specified by prescribing values which are related to the surface and bottom shear stresses.

The calculated velocity profile is displayed in Fig. 2 together with the experimental data. As can be seen the agreement is satisfactory. Further confidence in the calculated profile can be gained by plotting the profile on a logarithmic scale. If this is done one finds that the profile is well described by a straight line and thus that the profile is logarithmic. This logarithmic profile has been found in several experiments (Shemdin, 1972; Wu, 1975). The calculated eddy viscosity distribution is shown in Fig. 3. It is noted that the maximum non-dimensional eddy viscosity is the same as found in pipe and standard channel flows.

4. Application to the ocean surface layer

4.1. *Response to a suddenly imposed wind stress*

The first aspect of the ocean surface layer dynamics to be examined is that of the transient response of a quiescent ocean to an impulsively applied wind stress. This problem was considered already by Ekman (1905), who found that the surface drift current oscillates around a mean deflection angle of 45° to the right (Northern Hemisphere) of the wind direction. A constant eddy viscosity was however used in Ekman's analysis. Recently, Madsen (1977) has estimated the deflection angle to be of the order 10°, assuming the eddy viscosity to increase linearly from the surface.

A prediction of the development of the surface drift current, using the present model, has been carried out. The turbulence model for non-rotating flows was used, since the predicted result was found to be insensitive to the rotational effect. From Fig. 4 it is seen that the present model predicts an oscillating drift current around a mean deflection angle of the order 10°. This deflection angle is, however, depending on the roughness length of the surface, since a logarithmic velocity profile is assumed close to the surface. The angle 10° refers to a prescribed roughness length of 10^{-4} m which according to Kondo (1976) corresponds to a wind velocity of the order 7 m/s. Changing the roughness length within reasonable values will only

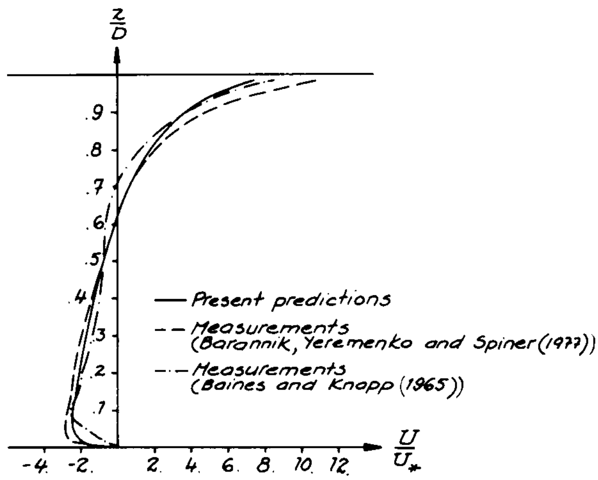

Fig. 2. The wind-induced channel flow. Comparison between predicted and measured mean velocity profiles.

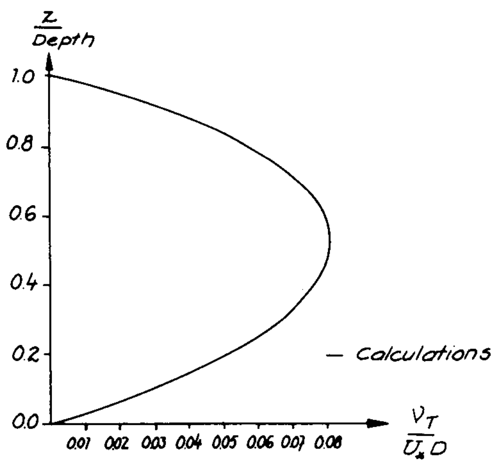

Fig. 3. The wind-induced channel flow. Calculated non-dimensional eddy viscosity distribution.

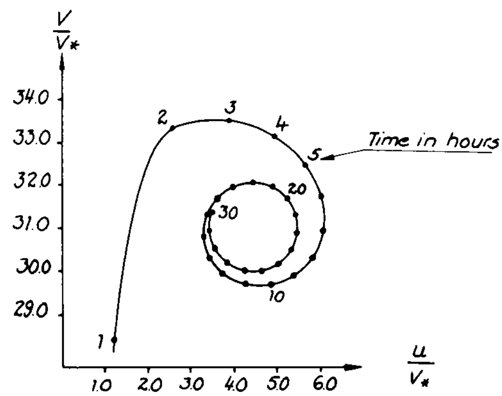

Fig. 4. The temporal development of the surface drift current due to a suddenly applied surface shear stress.

change the deflection angle a few degrees and the conclusion that the angle should be of the order 10° still holds. Further confidence in the predictions is gained from the calculated period of the oscillations, since this period is not a function of the eddy viscosity distribution. From Ekman's theory it is found to be 14.5 h for $f = 1.2 \cdot 10^{-4}\ s^{-1}$. From Fig. 4 it is seen that this is in perfect agreement with the model predictions. It may therefore be stated that the proposed model predicts a realistic development of the surface drift current even if a strict verification is out of reach.

4.2. *Steady state vertical distribution of mean flow and turbulence quantities*

It is realized that a steady state situation is never reached in the ocean surface layer. However, in order to be able to identify and analyse different variables only steady state distributions will be discussed in this section. The first question to be dealt with is how mean velocities are affected by different assumptions about the turbulence structure. Is it necessary to use an advanced turbulence model or will a suitably chosen constant eddy viscosity be sufficient? From Fig. 5 it is seen that the constant eddy viscosity solution is in good agreement with the one obtained with an advanced

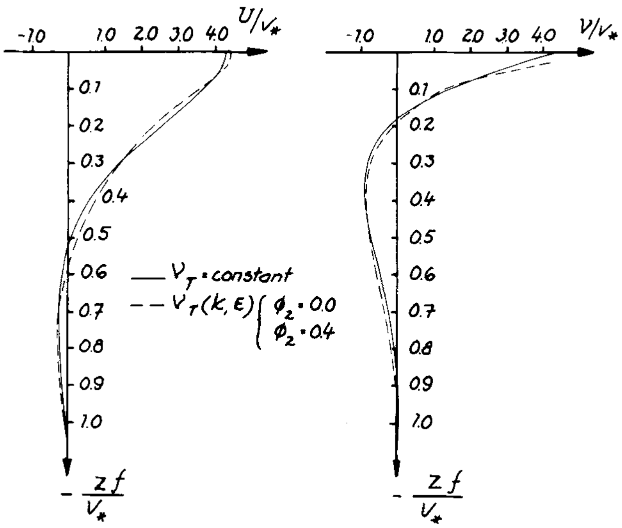

Fig. 5. The idealized Ekman layer. Mean velocity profiles as given by different turbulence models.

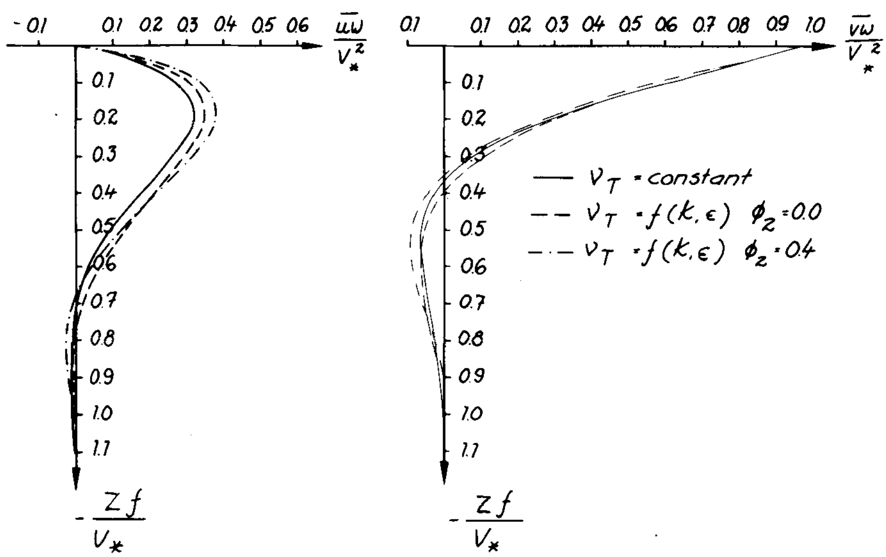

Fig. 6. The idealized Ekman layer. Shear stress distributions as predicted by different turbulence models.

turbulence model. The constant eddy viscosity was chosen as:

$$\nu_T = 0.026 V_x^2/f \tag{20}$$

where V_x is the surface friction velocity. An important difference between the two solutions is given in the near surface region. A constant viscosity implies that the velocity variation in the wind direction is linear, while the turbulence model assumes a logarithmic profile. This will of course result in different deflection angles for the surface drift current, as discussed earlier. The inclusion of the rotational effect in the turbulence model was found to affect the velocity profiles insignificantly.

The Reynolds stresses are, however, affected by the rotational effect as shown in Fig. 6. The maximum value of $\overline{uw}$ is increased by about 10% and $\overline{vw}$ is changed by about 40% at $zf/V_x =$

−0.55. The constant eddy viscosity solution is found to give a realistic distribution also of the Reynolds stresses.

Vertical distributions of turbulent kinetic energy and its dissipation rate are displayed in Fig. 7. The shape of these curves is the same as normally found in boundary layer flows, see Hinze (1959). Measurements of the dissipation rate in various aquatic systems have been collected by Dillon and Powell (1976). These data together with predictions for three different wind velocities are shown in Fig. 8. In these calculations a drag coefficient of $1.3 \cdot 10^{-3}$ and a Coriolis parameter of $1.0 \cdot 10^{-4}$ were assumed.

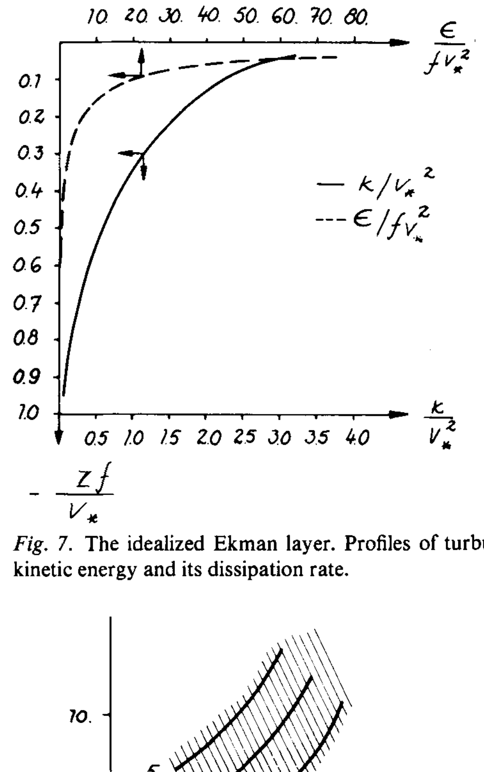

Fig. 7. The idealized Ekman layer. Profiles of turbulent kinetic energy and its dissipation rate.

Terms of the turbulent kinetic energy equation vs depth are shown in Fig. 9. Close to the surface there is a balance between production and dissipation while the diffusional transport contributes mainly in the deeper parts of the boundary layer. This kind of balance is also well known from general boundary layer theory. Eddy viscosity distributions calculated with and without the rotational term in the turbulence model are shown in Fig. 10. A similar eddy viscosity distribution is given by Shir (1973) for the atmospheric boundary layer.

Also for the steady state distributions it is interesting to compare the results with Madsen's (1977) analytical model. The depth of "practically no motion" is by Madsen's model estimated to $0.4v_*/f$ while the present model predicts the velocity at this depth to be about 3% of the surface velocity. From Fig. 5 it is seen that small velocities will be present down to $1.0\ v_*/f$ but Madsen's estimate is anyway regarded as being in agreement with the present predictions. A linearly increasing eddy-viscosity, as assumed by Madsen, is however basically unrealistic since the production of turbulence vanishes with vanishing velocity gradients. The eddy viscosity is thus bound to decrease in the outer region of the boundary layer, see Fig. 10. Close to the surface the eddy viscosity will, however, increase linearly and one may therefore conclude that Madsen's model is suitable for the near-surface region, while the model presented resolves the whole Ekman layer in a physically realistic manner.

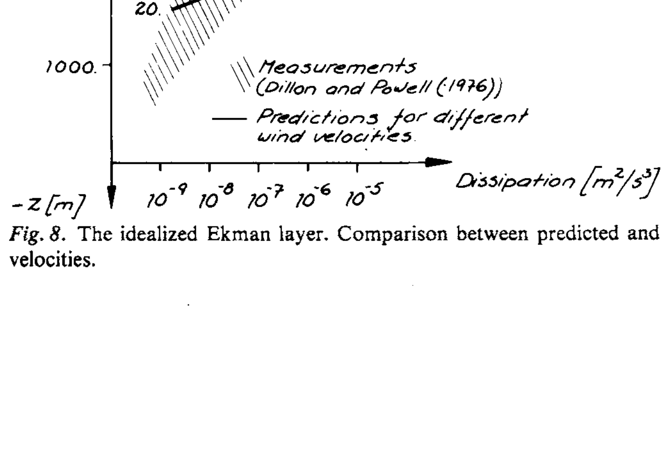

Fig. 8. The idealized Ekman layer. Comparison between predicted and measured dissipation rate for different wind velocities.

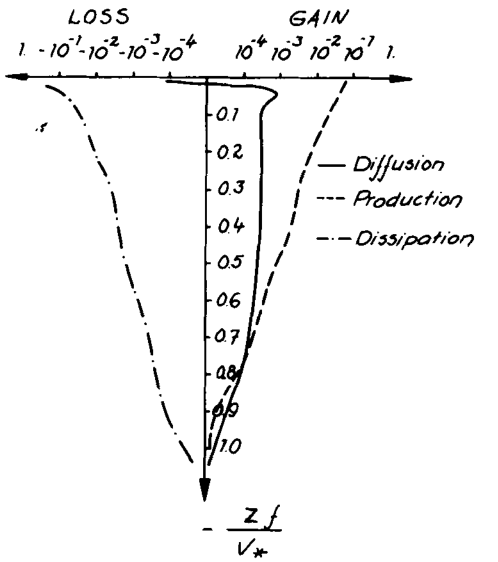

Fig. 9. The idealized Ekman layer. The relative importance of terms of the turbulent kinetic energy equation.

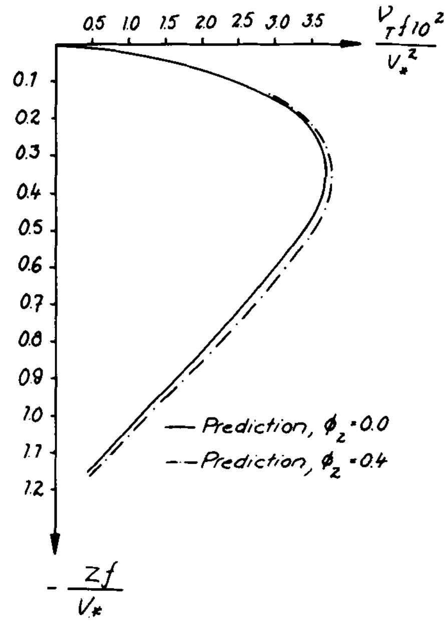

Fig. 10. The idealized Ekman layer. Eddy viscosity distributions as predicted with and without rotational effects in the turbulence model.

5. Discussion and conclusions

The main difficulty in verifying the above predictions is due to the lack of experimentally observed Ekman layers. According to Pollard (1977) this lack of observations is due to difficulties in making reliable measurements and the unsteadiness of the problem. It is unlikely that a steady state well-defined Ekman spiral will ever be observed. There are, however, two reasons for believing that the predictions presented give a realistic picture of the turbulent Ekman layer. Firstly, the mathematical model has, in this and other studies, been carefully verified against laboratory measurements of non-rotating flows. The model, and in particular the turbulence model, thus has proved to be able to represent the relevant physical processes accurately. Secondly, the inclusion of the Coriolis term in the momentum equations is straight-forward and does not introduce any uncertainty. The effect of rotation on the turbulence structure is analysed and found to be of minor importance. There is thus no reason to believe that the rotating boundary layer should be predicted less accurately than the non-rotating one.

The conclusions emerging from this study can be summarized by the following points:

(1) A suitably chosen constant eddy viscosity, Eq. (20), gives velocity and shear stress distributions in good agreement with those obtained with an advanced turbulence model.
(2) The $k - \varepsilon$ turbulence model has been extended to rotating flows. Eddy viscosity and shear stress distributions are found to be slightly modified by the rotational effect.
(3) Different turbulence quantities, characterizing the Ekman layer, are predicted and given in non-dimensional form. The Ekman layer is found to display the same features as boundary layers in general.
(4) The predicted eddy viscosity variation, Fig. 10, is recommended for studies of the vertical transport of different chemical and biological species. For large-scale hydrodynamical models, which use a constant vertical eddy viscosity, Eq. (20) is recommended.

Future work with the proposed model includes the extension to the stratified Ekman layer. Work in this direction, using the present model, has already been reported (Spalding and Svensson, 1976; Svensson, 1978a, b) but more applications are needed and currently undertaken.

6. Appendix

6.1. *Derivation of expressions for the Reynolds-stresses*

In this appendix an extension of the $k - \varepsilon$ model to flows exhibiting rotation will be derived. The starting point is the exact equation for the Reynolds stresses which reads:

$$\underbrace{\frac{D\overline{u_i u_j}}{Dt} = \mathrm{Diff}\,(\overline{u_i u_j})}_{\text{Diffusion}} \underbrace{- \left[\overline{u_j u_k}\frac{\partial U_i}{\partial x_k} + \overline{u_i u_k}\frac{\partial U_j}{\partial x_k}\right]}_{\text{Generation}}$$

$$\underbrace{- 2\nu \overline{\frac{\partial u_i}{\partial x_k}\frac{\partial u_j}{\partial x_k}}}_{\text{Dissipation}} \underbrace{+ \overline{\frac{p}{\rho}\left(\frac{\partial u_i}{\partial x_j} + \frac{\partial u_j}{\partial x_i}\right)}}_{\text{Pressure-strain}}$$

$$\underbrace{- f_l(e_{ilm}\overline{u_m u_j} + e_{jlm}\overline{u_m u_i}).}_{\text{Rotation}} \quad \text{(A1)}$$

This equation is, except for the rotational terms, given, for example, by Launder et al. (1975). In this equation f_l denotes the Coriolis vector, p pressure fluctuations, e_{ilm} the alternating tensor and $\mathrm{Diff}\,(\overline{u_i u_j})$ all diffusional processes. The equation is to be modelled according to the proposals by Gibson and Launder (1978). They did not, however, consider the Coriolis force; this term will be included in a way suggested by So (1977). In what follows the terms in (A1) are modelled term by term:

$$\frac{D\overline{u_i u_j}}{Dt} - \mathrm{Diff}(\overline{u_i u_j}) = 0. \quad \text{(A2)}$$

This assumption states that there is a local equilibrium between generation and dissipation terms. In the standard $k - \varepsilon$ model this equilibrium is assumed and if the extended version is to conform with the standard form it is necessary to make the above assumption. Note, however, that it is possible to relax this assumption and still stay within the two-equation framework, see Rodi (1976).

$$2\nu \overline{\frac{\partial u_i}{\partial x_k}\frac{\partial u_j}{\partial x_k}} = \tfrac{2}{3}\,\delta_{ij}\,\varepsilon \quad \text{(A3)}$$

which assumes the dissipative motions to be isotropic.

$$\overline{\frac{p}{\rho}\left(\frac{\partial u_i}{\partial x_j} + \frac{\partial u_j}{\partial x_i}\right)} = -C_1\frac{\varepsilon}{k}(\overline{u_i u_j} - \tfrac{2}{3}\delta_{ij}k) - C_2(P_{ij} - \tfrac{2}{3}\delta_{ij}P) - C_3(F_{ij} - \tfrac{2}{3}\delta_{ij}F) \quad \text{(A4)}$$

where

$$P_{ij} = -\left\{\overline{u_i u_k}\frac{\partial U_j}{\partial x_k} + \overline{u_j u_k}\frac{\partial U_i}{\partial x_k}\right\} \quad \text{(A5)}$$

$$F_{ij} = -f_l\left\{e_{ilm}\overline{u_m u_j} + e_{jlm}\overline{u_m u_i}\right\} \quad \text{(A6)}$$

$$P = -\overline{u_i u_k}\frac{\partial U_i}{\partial x_k} \quad \text{(A7)}$$

$$F = -f_l\, e_{ilm}\overline{u_m u_i}. \quad \text{(A8)}$$

The first two terms on the right-hand side of (A4) are given by Gibson and Launder (1978), while the last term has been proposed by So (1977). Free surface influence on pressure-strain has been neglected.

Collect terms and obtain:

$$0 = P_{ij} + F_{ij} - C_1\frac{\varepsilon}{k}(\overline{u_i u_j} - \tfrac{2}{3}\delta_{ij}k) - C_2(P_{ij} - \tfrac{2}{3}\delta_{ij}P) - C_3(F_{ij} - \tfrac{2}{3}\delta_{ij}F) - \tfrac{2}{3}\delta_{ij}\varepsilon \quad \text{(A9)}$$

which may be rearranged to

$$\overline{u_i u_j} = \frac{k}{C_1\varepsilon}\{P_{ij}(1 - C_2) + F_{ij}(1 - C_3) - \tfrac{2}{3}\delta_{ij}\varepsilon(1 - C_1 - C_2) + C_3\tfrac{2}{3}\delta_{ij}F\} \quad \text{(A10)}$$

where once again the local equilibrium assumption has been used. Only the vertical component of the rotation vector will be considered to be important in the present analysis, which means that F in the above expression equals zero. Further, f_3 will be denoted by f for short.

From (A10) the following individual stresses may be formulated:

$$\overline{u_1 u_3} = \frac{k}{\varepsilon}\left[\frac{1 - C_2}{C_1}\left(-\overline{u_3^2}\frac{\partial U_1}{\partial x_3}\right) + \frac{1 - C_3}{C_1}(f\overline{u_2 u_3})\right] \quad \text{(A11)}$$

$$\overline{u_2 u_3} = \frac{k}{\varepsilon}\left[\frac{1 - C_2}{C_1}\left(-\overline{u_3^2}\frac{\partial U_2}{\partial x_3}\right) - \frac{1 - C_3}{C_1}(f\overline{u_1 u_3})\right] \quad \text{(A12)}$$

$$\overline{u_3^2} = \tfrac{2}{3}k\left(\frac{C_1 + C_2 - 1}{C_1}\right). \tag{A13}$$

Introduce $\phi_1 = (1 - C_2)/C_1$; $\phi_2 = (1 - C_3)/C_1$ and $\phi_3 = 2(C_1 + C_2 - 1)/3C_1$.

By introducing (A12) and (A13) into (A11) the following expression for $\overline{uw}$ is obtained:

$$\overline{uw} = -\phi_1\phi_3\frac{k^2}{\varepsilon}\frac{\left(\dfrac{\partial U}{\partial z} + R\dfrac{\partial V}{\partial z}\right)}{1 + R^2}. \tag{A14}$$

And by introducing (A11) and (A13) into (A12) $\overline{vw}$ may be expressed as

$$\overline{vw} = -\phi_1\phi_3\frac{k^2}{\varepsilon}\frac{\left(\dfrac{\partial V}{\partial z} - R\dfrac{\partial U}{\partial z}\right)}{1 + R^2} \tag{A15}$$

where

$$R = \phi_2 f\frac{k}{\varepsilon}. \tag{A16}$$

From (8), (13) and (14) it is understood that the above expressions will only return to the standard $k - \varepsilon$ model for non-rotating flows if $\phi_1\phi_3$ is equal to C_μ. In fact, the constants given by Gibson and Launder (1978) give $\phi_1\phi_3 = 0.11$ while $C_\mu = 0.09$. For consistency, the product $\phi_1\phi_3$ will therefore be replaced by C_μ. The constant ϕ_2 is determined from a relationship given by So (1977). He determines ϕ_2 by postulating the Coriolis force effects to be similar to the centrifugal force effects due to surface curvature. Using this relationship gives $\phi_2 = 0.4$.

6.2. *Modification of terms in the k and ε equations*

The exact expression for generation of turbulent kinetic energy reads:

$$P = -\overline{u_j u_i}\frac{\partial U_i}{\partial x_j} \tag{A17}$$

for the present case thus:

$$P = -\overline{uw}\frac{\partial U}{\partial z} - \overline{vw}\frac{\partial V}{\partial z}. \tag{A18}$$

If (A14) and (A15) are introduced into (A18), the result is:

$$P = C_\mu\frac{k^2}{\varepsilon}\left[\left(\frac{\partial U}{\partial z}\right)^2 + \left(\frac{\partial V}{\partial z}\right)^2\right]/(1 + R^2) \tag{A19}$$

which is the modified expression for P. In the ε-equation it is $P\varepsilon/k$, that specifies the production term. The modification of the production term in the ε-equation is thus analog.

The exact expression for diffusion of k reads:

$$\frac{\partial}{\partial x_j}\left(\frac{\overline{pu_j}}{\rho_0} + \overline{u_j k'} - \nu\left(\frac{\partial k}{\partial x_j} + \frac{\partial}{\partial x_i}\overline{u_i u_j}\right)\right) \tag{A20}$$

where p denotes pressure fluctuations and k' the instantaneous value of k. In the modelling of this expression it is customary to consider only the term containing k'. For the present case thus:

$$\frac{\partial}{\partial x_3}\overline{(u_3 k')}. \tag{A21}$$

Since the expression for $\overline{u_3^2}$ (A13) does not show any explicit dependence on rotation it is assumed that the diffusion term needs no modification.

REFERENCES

Baines, W. D. and Knapp, D. J. 1965. Wind driven water currents. *J. Hydr. Div.* ASCE, HY2, 205–221.

Barannik, V. A., Yeremenko, Ye. V. and Spiner, O. M. 1977. Determination of eddy viscosity and friction at the bottom in wind-driven currents in shallow water basins. *Fluid Mech. 6*, 165–172.

Chou, P. Y. 1945. On the velocity correlations and the solution of the equations of turbulent fluctuation. *Q. appl. Math. 3*, 38–54.

Deardorff, J. W. 1970. A three-dimensional numerical investigation of the idealized planetary boundary layer. *Geophys. Fluid Dyn. 1*, 377–410.

Dillon, T. M. and Powell, T. M. 1976. Low-frequency turbulence spectra in the mixed layer of Lake Tahoe, California-Nevada. *J. Geophys. Res. 81*, 6421–6427.

Ekman, W. V. 1905. On the influence of the earth's rotation on ocean currents. *Ark. Mat. Astr. Fys. 2*, 1–53.

Gibson, M. M. and Launder, B. E. 1978. Ground effects on pressure fluctuations in the atmospheric boundary layer. *J. Fluid Mech. 86, part 3*, 491.

Hinze, J. O. 1959. *Turbulence.* New York, Toronto, London: McGraw-Hill.

Hussain, A. K. M. F. and Reynolds, W. C. 1975. Measurements in fully developed turbulent channel flow. *J. Fluids Eng. Dec.* 568–578.

Kondo, J. 1976. Parameterization of turbulent transport in the top meter of the ocean. *J. Phys. Oceanogr. 6*, 712–720.

Launder, B. E., Reece, G. J. and Rodi, W. 1975.

Progress in the development of a Reynolds-stress turbulence closure. *J. Fluid Mech. 68*, 537–566.
Launder, B. E. and Spalding, D. B. 1972. *Mathematical models of turbulence*. London and New York: Academic Press.
Launder, B. E. and Spalding, D. B. 1974. The numerical computation of turbulent flows. *Comput. Methods Appl. Mech. & Eng. 3*, 269–288.
Madsen, O. S. 1977. A realistic model of the wind-induced Ekman boundary layer. *J. Phys. Oceanogr. 7*, 248–255.
Marchuk, G. I., Kochergin, V. P., Klimok, V. I. and Sukhorukov, V. A. 1977. On the dynamics of the ocean surface mixed layer. *J. Phys. Oceanogr. 7*, 865–875.
Mellor, G. L. and Durbin, P. A. 1975. The structure and dynamics of the ocean surface mixed layer. *J. Phys. Oceanogr. 5*, 718–728.
Mellor, G. L. and Yamada, T. 1974. A hierarchy of turbulence closure models for planetary boundary layers. *J. Atmos. Sci. 31*, 1791–1806.
Mellor, G. L. and Yamada, T. 1977. A turbulence model applied to geophysical problems. Symposium on turbulent shear flows. Pennsylvania Univ.
Pollard, R. T. 1977. Observations and models of the structure of the upper ocean. In *Modelling and prediction of the upper layers of the ocean* (ed. E. B. Krauss), Pergamon Press.
Rodi, W. 1976. A new algebraic relation for calculating the Reynolds stresses. *Z. angew. Math. Mech. 56*, 219–221.
Rodi, W. 1978. Turbulence models and their application in hydraulics. A state of the art review. SFB 80/T/127. Universität Karlsruhe.
Shemdin, O. H. 1972. Wind-generated current and phase speed of wind waves. *J. Phys. Oceanogr. 2*, 411–419.
Shir, C. C. 1973. A preliminary numerical study of atmospheric turbulent flows in the idealized planetary boundary layer. *J. Atmos. Sci. 30*, 1327–1339.
Singhal, A. K. and Spalding, D. B. 1975. Prediction of two-dimensional boundary layers with the aid of $k-\varepsilon$ model of turbulence. Heat Transfer Section Report, HTS/75/15, Mech. Eng. Imperial College, London.
So, R. M. 1977. On model constants and second order closure for curved shear flows. *Appl. Sci. Res. 33*, 353–368.
Spalding, D. B. and Svensson, U. 1976. *The development and erosion of the thermocline, in Turbulent Buoyant Convection* (ed. D. B. Spalding), Washington, D.C.: Hemisphere Publishing Corp.
Svensson, U. 1978a. A mathematical model of the seasonal thermocline. Report No. 1002. Dept. of Water Resources Eng. Univ. of Lund, Sweden.
Svensson, U. 1978b. Examination of the summer stratification. *Nord. Hydrol. 9*, 105–120.
Wu, J. 1975. Wind-induced drift currents. *J. Fluid Mech. 68*, 49–70.
Wyngaard, J. C. 1975. Modeling the planetary boundary layer—Extension to the stable case. *Boundary-Layer Meteorol. 9*, 441–460.
Zeman, O. and Tennekes, H. 1975. A self-contained model for the pressure terms in the turbulent stress equations of the neutral atmospheric boundary layer. *J. Atmos. Sci. 32*, 1808–1813.

СТРУКТУРА ЭКМАНОВСКОГО ТУРБУЛЕНТНОГО СЛОЯ

Для анализа структуры однородного приповерхностного слоя океана используется математическая модель. Модель проверяется по данным лабораторных измерений полностью развитого потока в канале и потока в канале, вызываемого ветром. Используются и обсуждаются турбулентные модели различной сложности. Получено и проверено обобщение k–ε модели турбулентности для вращающихся потоков.

Исследование показывает, что подходящим образом выбранная постоянная турбулентная вязкость адэкванта для предсказания распределений скорости и сдвиговых напряжений в экмановском слое. Однако для переноса различных химических и биологических субстанций необходимо знать детальные турбулентные характеристики слоя. Поэтому получены и проанализированы безразмерные вертикальные распределения различных турбулентных величин, характеризующих экмановский слой. Найдено, что эффекты вращения в некоторой мере изменяют в модели распределение напряжения сдвига в более глубоких частях пограничного слоя.